

Induced charge-density oscillations at metal surfaces

V. M. Silkin ^{a,*}, I. A. Nechaev ^a, E. V. Chulkov ^{a,b}, and
P. M. Echenique ^{a,b}

^a*Donostia International Physics Center (DIPC), P. de Manuel Lardizabal 4,
20018 San Sebastián, Basque Country, Spain*

^b*Departamento de Física de Materiales, Facultad de Ciencias Químicas,
UPV/EHU and Centro Mixto CSIC-UPV/EHU, Apdo. 1072, 20080 San
Sebastián, Basque Country, Spain*

Abstract

Induced charge-density (ICD) oscillations at the Cu(111) surface caused by an external impurity are studied within linear response theory. The calculation takes into account such properties of the Cu(111) surface electronic structure as an energy gap for three-dimensional (3D) bulk electrons and a $s - p_z$ surface state that forms two-dimensional (2D) electron system. It is demonstrated that the coexistence of these 2D and 3D electron systems has profound impact on the ICD in the surface region. In the case of a static impurity the characteristic ICD oscillations with the $1/\rho^2$ decay as a function of lateral distance, ρ , are established in both electron systems. For the impurity with a periodically time-varying potential, the novel dominant ICD oscillations which fall off like $\sim 1/\rho$ are predicted.

Key words: Surface electronic phenomena, Noble metals, Low index single metal surfaces, Electronic surface states, Adsorbates

In the last years, scanning tunneling microscopy has become a powerful tool to study phenomena governed by screening at metal surfaces, i.e., charge rearrangement in response to the disturbance caused by impurities or defects [1,2,3,4,5,6,7,8,9,10]. Remarkable examples of that are the visualization of surface-state-originated Friedel oscillations of the induced charge-density (ICD) at metal surfaces [1,2] and the investigation of the indirect long-range interaction between adsorbates mediated by these oscillations [11]. It has been demonstrated [12,13] that at noble-metal (111) surfaces this interaction, whose

* Corresponding author. Tel.: +34 943 018284; Fax.: +34 943 015600
Email address: waxslavs@sc.ehu.es (V. M. Silkin).

energy decays as $1/\rho^2$ with the lateral distance ρ between adsorbates, can lead to mutual redistribution of adsorbed atoms up to $\rho \sim 10$ nm. This interaction might also be responsible for the rearrangement of adsorbate species on the Si(111)- $\sqrt{3} \times \sqrt{3}$ -Ag surface [14]. Moreover, very recently it has been reported on a realization of a self-assembled two-dimensional (2D) atomic structure due to this interaction [15].

In the theoretical studies of such phenomena, the scattering approach has found the wide application [12,16,17,18]. Within this approach, a $s-p_z$ surface state at the noble-metal (111) surfaces is considered to form a 2D free electron gas, ignoring the fine structure of the surface-state wave function and the fact that this 2D electron gas *coexists* with underlying three-dimensional (3D) electron system. It is well known that the 2D electron system responds to the introduction of an impurity by producing Friedel oscillations with the characteristic $1/\rho^2$ decay [19], whereas in the 3D electron gas the oscillations fall off as $1/R^3$, R being a distance from the impurity [20]. Nevertheless, up to date, the question of how the 2D and 3D systems respond *simultaneously* in the vicinity of a metal surface has not been addressed yet. An answer can be obtained, in principle, from *ab initio* calculations. But, at present, these evaluations are feasible only for systems with the lateral distances between adsorbates of the order of several Å [21].

In this Letter we investigate the response of an electron system at a metal surface to the introduction of an impurity, considering the Cu(111) surface as an example. We show that taking explicitly into account the realistic Cu(111) surface band structure, which is characterized by the energy gap at the center of surface Brillouin zone (SBZ) and the $s-p_z$ partly occupied surface state, is crucial for the description of the surface response.

In order to evaluate the ICD, we adopt an approach based on linear response theory in which an external perturbation $V_{ext}(\mathbf{r}'; \omega)$ and the corresponding ICD $n_{ind}(\mathbf{r}; \omega)$ are related by the equation

$$n_{ind}(\mathbf{r}; \omega) = \int d\mathbf{r}' \chi(\mathbf{r}, \mathbf{r}'; \omega) V_{ext}(\mathbf{r}'; \omega). \quad (1)$$

Here $\chi(\mathbf{r}, \mathbf{r}'; \omega)$ is the density-response function which is non-local and complex and contains information on electronic excitations. In time-dependent density functional theory $\chi(\mathbf{r}, \mathbf{r}'; \omega)$ satisfies the integral equation [22]

$$\chi = \chi^0 + \chi^0(v_c + K_{xc})\chi \quad (2)$$

with $\chi^0(\mathbf{r}, \mathbf{r}'; \omega)$ being the response function of a noninteracting electron system, $v_c(\mathbf{r}-\mathbf{r}')$ is the Coulomb potential, and $K_{xc}(\mathbf{r}, \mathbf{r}'; \omega)$ accounts for dynamical exchange-correlation effects. As we are mainly interested in the evaluation

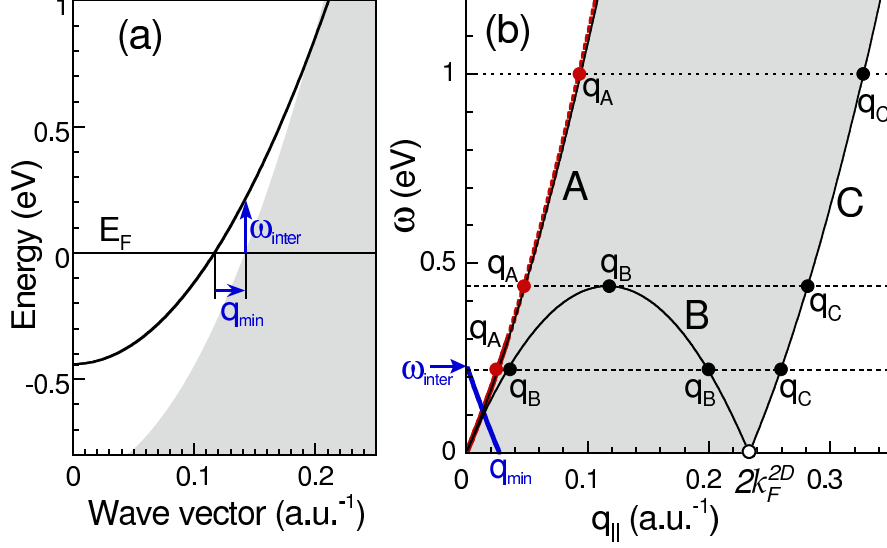


Fig. 1. (a) Surface electronic structure of Cu(111). The grey area represents the projected bulk electronic structure. Solid line shows the surface state dispersion with an effective mass of $m^* = 0.42m_e$. (b) The phase space available for $e - h$ excitations. In the grey area the surface state intraband $e - h$ excitations are permitted. The intraband $e - h$ bulk excitations are possible everywhere. The interband “surface state—bulk” transitions are forbidden in the area below the blue line. Lines A, B, and C are respectively described by equations $\omega = v_F^{2D} q_{||} + q_{||}^2/2m^*$, $\omega = v_F^{2D} q_{||} - q_{||}^2/2m^*$, and $\omega = -v_F^{2D} q_{||} + q_{||}^2/2m^*$ with v_F^{2D} being the 2D (surface state) Fermi velocity. Red line shows the acoustic surface plasmon (ASP) dispersion [27] very close to the line A (solid red line corresponds to the well defined ASP, whereas dashed one indicates the region of its gradual degradation).

of long-range charge density oscillations, we use the random phase approximation, i.e., $K_{xc} = 0$. The inclusion of a non-zero K_{xc} mainly affects the amplitude of Friedel oscillations [23,24,25].

To describe the Cu(111) surface, we employ a slab containing 81 atomic layers of Cu together with a vacuum region corresponding to 20 interlayer spacings. The substrate is described by a model one-dimensional potential of Ref. [26]. This potential reproduces the key ingredients of the Cu(111) electronic structure shown in Fig. 1(a), namely, the energy gap at the center of the SBZ and the $s - p_z$ surface and image-potential states in it. Using translation invariance parallel to the surface, one can perform the 2D Fourier transform for all quantities in Eq. (1). The ICD has now the following form [23]

$$n_{ind}(\rho, z; \omega) = \frac{1}{2\pi} \int_0^\infty dq_{||} q_{||} J_0(q_{||}\rho) n_{ind}(q_{||}, z; \omega), \quad (3)$$

$$n_{ind}(q_{||}, z; \omega) = \int dz' \chi(q_{||}, z, z'; \omega) V_{ext}(q_{||}, z'; \omega), \quad (4)$$

where $V_{ext}(q_{||}, z'; \omega)$ is the 2D Fourier transform of an external potential, J_0 is the Bessel function of order 0, and z (ρ) is a distance perpendicular (parallel) to the surface. χ^0 is given by¹

$$\begin{aligned} \chi^0(q_{||}, z, z'; \omega) = & 2 \sum_{i,j} \phi_i(z) \phi_j^*(z) \phi_j(z') \phi_i^*(z') \\ & \times \int \frac{d\mathbf{k}_{||}}{(2\pi)^2} \frac{f_{i,\mathbf{k}_{||}+\mathbf{q}_{||}} - f_{j,\mathbf{k}_{||}}}{E_{i,\mathbf{k}_{||}+\mathbf{q}_{||}} - E_{j,\mathbf{k}_{||}} + \omega + i\eta}, \end{aligned} \quad (5)$$

where the sum runs over the bands i and j , f 's are the Fermi factors, $E_{i,\mathbf{k}_{||}+\mathbf{q}_{||}} = \varepsilon_i + (\mathbf{k}_{||} + \mathbf{q}_{||})^2/2m_i^*$, $E_{j,\mathbf{k}_{||}} = \varepsilon_j + \mathbf{k}_{||}^2/2m_j^*$. ε_i (ϕ_i) represent the one-particle energies (wave functions) obtained with the model potential [26]. The experimental values of effective masses m_i^* different from the free electron mass have been used in Eq. (5). The regions of possible electron-hole ($e-h$) excitations at Cu(111) are shown in Fig. 1(b). In the calculation of χ^0 , a finite value for the broadening parameter $\eta = 0.001$ eV was introduced.

We begin with the case of response to a static external potential of the form

$$V_{ext}(\mathbf{r}) = -Qe/|\mathbf{r} - \mathbf{r}_0|, \quad (6)$$

caused by an impurity of charge $Qe = 1$ placed at $\mathbf{r}_0 = \{\mathbf{r}_{||} = 0, z_0\}$.² Fig. 2(a) shows the obtained ICD multiplied by $\rho^2 + (z - z_0)^2$ as a function of z and ρ . One can see that in a horizontal plane the Friedel oscillations peculiar to 2D electron systems are nicely reproduced: the ICD amplitude shows the quadratic dependence on ρ in the lateral direction and the period of the oscillations is precisely determined by the Fermi wave vector of the surface state, $k_F^{2D} = 0.1165$ a.u. In the direction perpendicular to the surface the ICD oscillations demonstrate the behavior more complicated than that expected for a 3D electron gas. Note also that any displacement of the impurity along the z -direction in the vicinity of the crystal border changes only the amplitude of the oscillations but not their character.

To reveal the importance of the 3D system for the ICD shown in Fig. 2(a), we consider a hypothetical case of a free standing surface state without bulk electrons (the case of a pure 2D electron gas). Fig. 2(b) shows the resulting ICD. As in Fig. 2(a), one can observe the 2D Friedel oscillations in the lateral direction, while in the perpendicular direction the ICD behavior is in clear correspondence with the location of surface-state charge-density presented in Fig. 2(c). However, there is a qualitative difference between the oscillations presented in Figs. 2(a) and 2(b): the ICD as a function of z in Fig. 2(a)

¹ Hartree atomic units are used throughout unless otherwise is stated.

² In all figures, the impurity was placed at $z_0 = 1.97$ a.u.

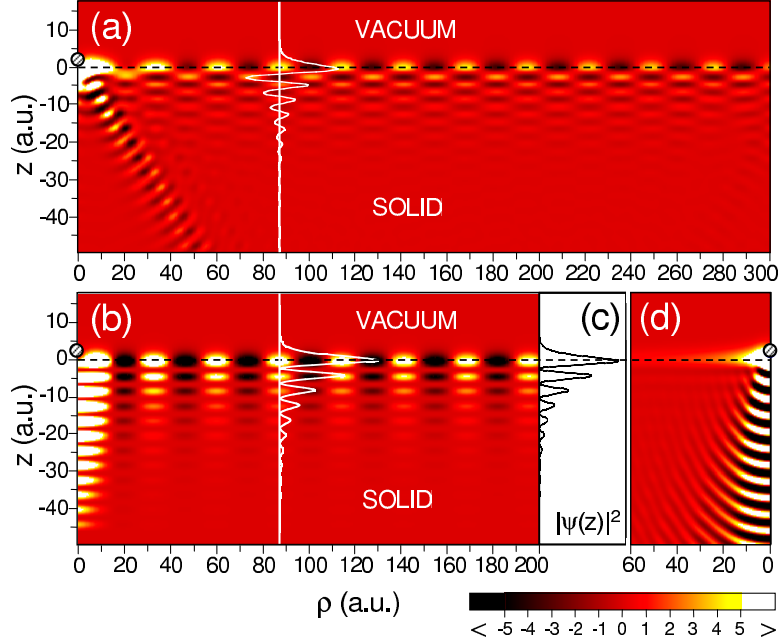


Fig. 2. (a) Map of $n_{ind} \times (\rho^2 + (z - z_0)^2)$ (in a.u. $\times 10^5$) induced by an impurity placed at the point shown by shaded circle as a function of z and ρ . Horizontal dashed line shows the crystal border. The solid (vacuum) is located for $z < 0$ ($z > 0$). The surface atomic layer is at $z = -1.97$ a.u. (b) The same as in (a) for a hypothetical case of a free standing surface state without bulk electrons. Additionally, in (a, b) $n_{ind} \times (\rho^2 + (z - z_0)^2)$ as a function of z is shown by white curves for the vertical cut $\rho = 87$ a.u. (c) The surface state charge density as a function of z . (d) Shows the same as in (a) for the jellium model. Note the absence of lateral ICD oscillations in this case.

changes sign whereas in the pure 2D case it does not occur (see white curves in Figs. 2(a) and (b) which give the ICD along the vertical cut $\rho = 87$ a.u.). Similar behavior is observed for any ρ . Inspecting Fig. 2(a), one can see that the $\sim 1/\rho^2$ decay takes place both in the 2D electron system and in the region of the 3D system adjacent to the crystal border. In the latter system for a given z the ICD oscillates with the opposite sign to that in the 2D one. To clarify the origin of this ICD behavior we separate contributions to χ_0 in Eq. (5) into three parts: "surface state—surface state" ($s-s$), "bulk—bulk" ($b-b$), and "surface state—bulk" ($s-b$) transitions

$$\chi^0(q_{||}, z, z'; \omega) = \sum_{\alpha} \chi_{\alpha}^0(q_{||}, z, z'; \omega), \quad (7)$$

where α stands for $s-s$, $b-b$, or $s-b$, and the summation is performing over these three components. As a result, the ICD of Eq. (4) can be rewritten as the sum of the partial ICD concerned with the contributions of the 2D and 3D systems as well as their mixing

$$n_{ind}(q_{||}, z; \omega) = \sum_{\alpha} n_{ind}^{\alpha}(q_{||}, z; \omega), \quad (8)$$

where

$$n_{ind}^{\alpha}(q_{||}, z; \omega) = \int dz' \chi^{\alpha}(q_{||}, z, z'; \omega) \{V_{ext}(q_{||}, z'; \omega) + \int dz'' v_c(q_{||}, z', z'') \sum_{\beta \neq \alpha} n_{ind}^{\beta}(q_{||}, z''; \omega)\}. \quad (9)$$

Here $v_c(q_{||}, z', z'') = \frac{2\pi}{q_{||}} e^{-q_{||}|z'-z''|}$ is the 2D Fourier transform of the bare Coulomb interaction, each χ^{α} is defined through Eq. (2) by the corresponding χ_{α}^0 .

Thus, the ICD shown in Fig. 2(a) comprises three interrelated components n_{ind}^{α} which represent the response of the corresponding “subsystems” to both the external perturbation (6) and the electrostatic field created by the two other n_{ind}^{β} . Note that if we neglect the χ_{s-b}^0 term in Eq. (7) and approximate the surface-state wave function by the δ -function, we obtain the results of Ref. [28]. The main advantage of Eq. (9) over Eq. (4) is the possibility to solve it iteratively and to analyze step-by-step how one component affects the rest and vice versa. Actually, by setting $n_{ind}^{b-b} = n_{ind}^{s-b} = 0$, we find n_{ind}^{s-s} shown in Fig. 2(b). It can be considered as a first iteration. Then, by substituting the obtained n_{ind}^{s-s} into n_{ind}^{b-b} with $n_{ind}^{s-b} = 0$, we find the response of the 3D system to the external field and the field created by the ICD of Fig. 2(b), and so on. It explains why the $\sim 1/\rho^2$ decay of the ICD peculiar to the 2D system takes also place in the 3D electron system adjacent to the crystal border. Additionally the screening by the 3D system of the complex perturbation mentioned above is the origin of an alternate behavior of the ICD as a function of z at a given ρ (see the white line in Fig. 2(a)).

To emphasize the role of the realistic electronic structure in the surface response, we plot in Fig. 2(d) the ICD obtained within a jellium model for $r_s = 2.67$ commonly used for description of Cu *sp*-valence electrons. In this case the distinct behavior of n_{ind} along the crystal surface without any oscillations is clearly seen. Instead, this model gives strong ICD oscillations in the direction perpendicular to the surface which are suppressed in the realistic consideration (Fig. 2(a)) due to complicated mutual influence of one “subsystem” on the others.³ Also, at small ρ , this influence leads to the ICD penetrating into the bulk only along a straight line at a finite angle away from the surface normal. Similar effect has also been observed in the studies of long-lived adsorbate-induced states at metal surfaces [29,30].

Now we consider the case of the potential (6) varying in time with some small frequency ω_0 as $\cos(\omega_0 t)$. As we deal with the linear system, the superposition principle would hold true. Therefore, once the response to the given potential

³ More detailed analysis will be given elsewhere.

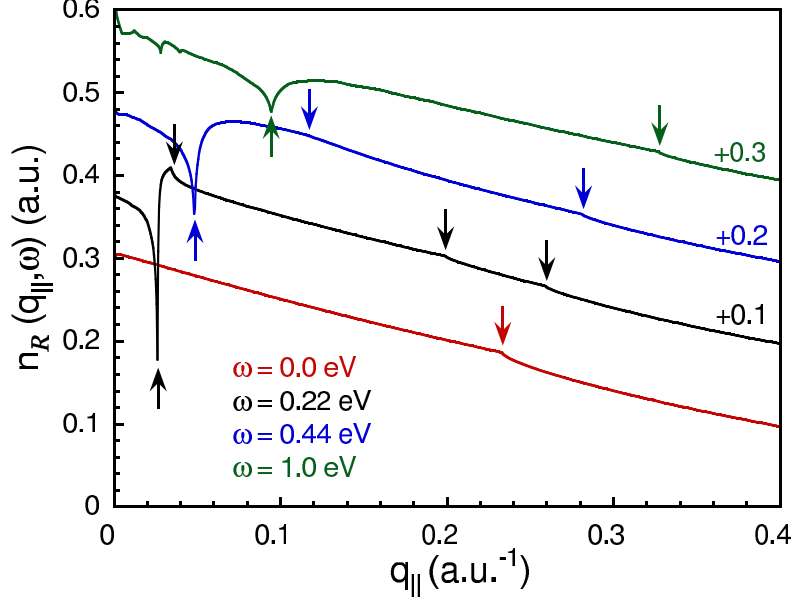


Fig. 3. $n_R(q_{\parallel}, z = 0; \omega_0)$ vs q_{\parallel} for four values of ω_0 . n_R for $\omega_0 = 0.22$ eV, 0.44 eV, and 1.0 eV are displaced vertically by 0.1, 0.2, and 0.3 a.u., respectively. The arrows \uparrow (\downarrow) indicate the singularities positions at q_A ($q_{B,C}$).

is known, the response to an arbitrary time-varying external potential can be evaluated. In contrast to the previous static case when the integration in Eq. (3) over q_{\parallel} is performed along the line $\omega = 0$ of Fig. 1(b), here the integration should be performed along the line $\omega = \omega_0$. Moreover, in this case the ICD depends on time and has the following form

$$\begin{aligned} n_{ind}(\rho, z; t) &= n_R(\rho, z; \omega_0) \cos(\omega_0 t) + n_I(\rho, z; \omega_0) \sin(\omega_0 t) \\ &= A(\rho, z; \omega_0) \cos(\omega_0 t - \theta(\rho, z; \omega_0)) \end{aligned}$$

where $n_R(\rho, z; \omega_0)$ and $n_I(\rho, z; \omega_0)$ are defined through Eqs. (3) and (4) by the real and imaginary parts of the response function $\chi(q_{\parallel}, z, z'; \omega_0)$, respectively. The ICD amplitude is $A = \sqrt{n_R^2 + n_I^2}$ and the phase shift θ is defined by $\tan(\theta) = n_I/n_R$. Thus, a non-vanishing n_I leads to a non-zero phase shift between the ICD and external perturbation oscillations (it means an energy absorption in the electron system).

Fig. 1(b) shows, as an example, three lines corresponding to $\omega_0 = 0.22$ eV, 0.44 eV, and 1.0 eV. Contrary to the “static” $\omega_0 = 0$ line which has only one singularity point at $q_{\parallel} = 2k_F^{2D}$ ensuring the Friedel oscillations in n_{ind} with the $1/\rho^2$ decay, the $\omega_0 \neq 0$ lines have up to four singularity points (labeled by $q_{A,B,C}$) due to the singularities at lines A, B, and C [31], what makes the dynamic response more complex. Commonly, these singularities are similar to that at $q_{\parallel} = 2k_F^{2D}$ in the static case. But, at the Cu(111) surface the q_A singularity corresponds to the location of the acoustic surface plasmon

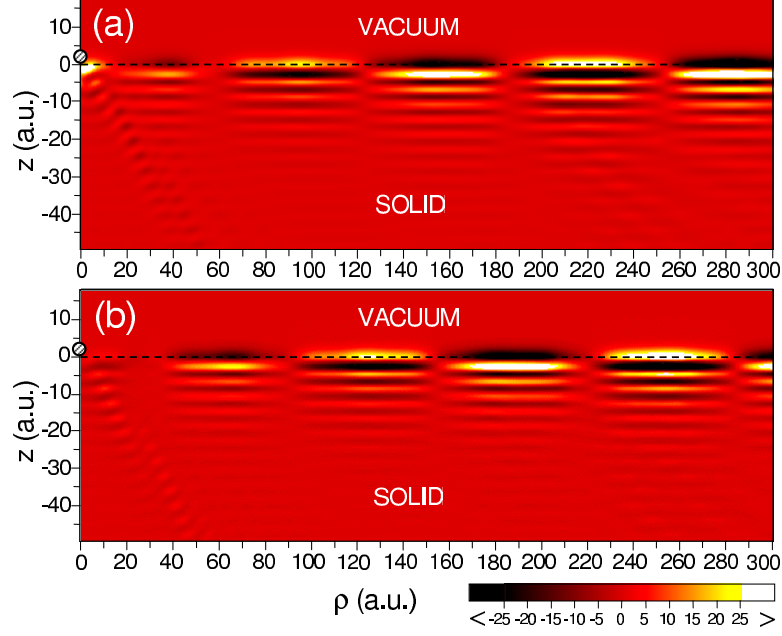


Fig. 4. Map of n_R (a) and n_I (b) induced by the time-varying external perturbation (6) with frequency $\omega_0 = 0.44$ eV as a function of z and ρ and multiplied by $\rho^2 + (z - z_0)^2$. Note the enhanced scale comparing with the one of Fig. 2. Other notions are the same as in Fig. 2(a).

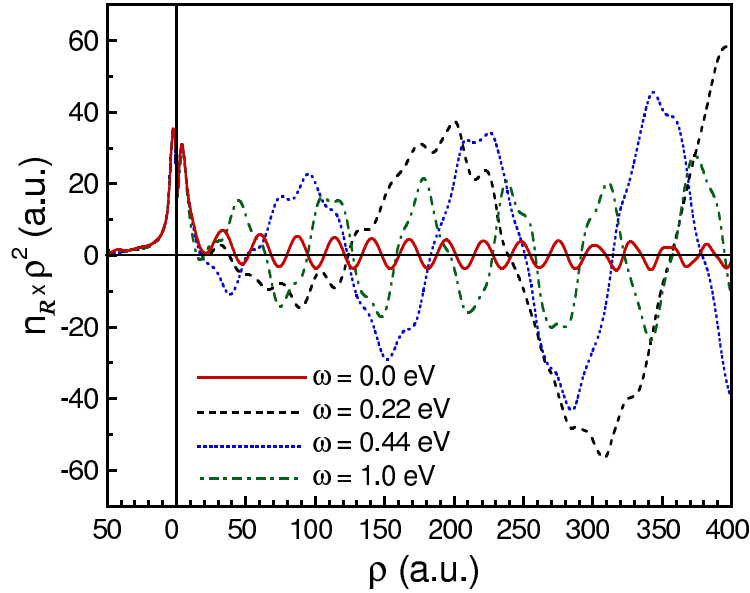


Fig. 5. $n_R(\rho, z = 0; \omega_0)$ multiplied by ρ^2 vs ρ for $\omega_0 = 0.0$ eV, 0.22 eV, 0.44 eV, and 1.0 eV. On the left of the vertical line $\rho = 0$, the corresponding curves in the jellium model do not show any oscillations.

(ASP) (see Fig. 1(b)), whose origin and nature has recently been studied [27,28]. The ASP singularity, appearing due to the coexistence of 2D and 3D electron systems [28], is much stronger than the other ones and leads to the $\sim \cos(q_A \rho)/\rho$ -like oscillations, i.e., with the spatial decay inversely

proportional to ρ only. To visualize the distinct nature of singularities at q_A and $q_{B,C}$, the dependence of n_R on $q_{||}$ for $z = 0$ is shown in Fig. 3.

Fig. 4 represents the ICD components n_R (ICD at the moment $t = 2n\pi/\omega_0$, n is integer) and n_I ($t = (2n + 1/2)\pi/\omega_0$) for $\omega_0 = 0.44$ eV. One can clearly see that in this case the ICD along the surface is dominated by oscillations with q_A wave vector corresponding to the ASP. Nevertheless, the ICD also contains contributions originated from the other two singularity points, q_B and q_C . In general, the structure of the resulting oscillations is quite complicated, but fitted rather well by three cos-like functions. To compare the decay law of oscillations, we show $n_R(\rho, z = 0; \omega_0)$ for $\omega_0 = 0.0$ eV, 0.22 eV, 0.44 eV, and 1.0 eV in Fig. 5.⁴ For small ω_0 , the oscillations in 2D with $q_A = \omega_0/v_F^{2D}$ have the $\sim \cos(q_A\rho)/\rho$ asymptotic behavior. The same kind of ICD oscillations arises in the 3D system in the proximity of the 2D electron one. As ω_0 increases, the ASP loses its strength due to interband transitions (see Figs. 1(b) and 3), and oscillations with q_A gradually change their decay behavior from ρ^{-1} to ρ^{-2} . Thus, for $\omega_0 = 0.22$ eV the decay obeys the ρ^{-1} law, while it is proportional to $\rho^{-1.4}$ for $\omega_0 = 0.44$ eV, and $\rho^{-1.7}$ for $\omega_0 = 1.0$ eV.

In conclusion, we nicely reproduce within linear response theory the Friedel oscillations of the ICD at the Cu(111) surface caused by a static impurity, taking explicitly into account the realistic surface band structure. It is shown that the coexistence of the 2D electron system with the 3D one has profound impact on the screening properties at the metal surface. Thus, additionally to the $\sim \cos(k_F^{2D}\rho)/\rho^2$ ICD oscillations in the 2D system along the surface, the same kind of oscillations occurs in the 3D electron system in the region adjacent to the crystal border. In the case of a time-varying potential, dominant $\cos(\omega_0/v_F^{2D} \cdot \rho)/\rho$ -like oscillations at the surface in both the 2D and 3D electron systems are predicted for low frequencies. We expect that these oscillations can lead to a longer-range indirect interaction between atoms and molecules at metal surfaces than it is thought nowadays.

Acknowledgments

The authors thank A. Arnau and I. Nagy for useful discussions. We acknowledge partial support by the University of the Basque Country, the Departamento de Educación del Gobierno Vasco, MCyT (Grant No. MAT 2001-0946) and the European FP6 Network of Excellence (FP6-NoE NANOQUANTA (500198-2)).

⁴ Some distortion seen in the $\omega_0 = 0$ ICD for $\rho \geq 300$ a.u. is explained by finite size of the slab. An increase of the slab thickness moves gradually this disturbance region farther away in ρ .

References

- [1] M.F. Crommie, C.P. Lutz, and D.M. Eigler, *Science* **262** (1993) 218.
- [2] Y. Hasegawa and P. Avouris, *Phys. Rev. Lett.* **71** (1993) 1071.
- [3] P.T. Sprunger, L. Petersen, E.W. Plummer, E. Lægsgaard, and F. Besenbacher, *Science* **275** (1997) 1764.
- [4] Ph. Hofmann, B.G. Briner, M. Doering, H.-P. Rust, E.W. Plummer, and A.M. Bradshaw, *Phys. Rev. Lett.* **79** (1997) 265.
- [5] E. Wahlström, I. Ekwall, H. Olin, and L. Walldén, *Appl. Phys. A* **66** (1998) S1107.
- [6] N. Sato, S. Takeda, T. Nagao, and S. Hasegawa, *Phys. Rev. B* **59** (1999) 2035.
- [7] A. Begicevic, S. Ovesson, P. Hyldgaard, B.I. Lundqvist, H. Brune, and D.R. Jennison, *Phys. Rev. Lett.* **85** (2000) 1910.
- [8] H.C. Manoharan, C.P. Lutz, and D.M. Eigler, *Nature (London)* **403** (2000) 512.
- [9] N. Nilius, T.M. Wallis, M. Persson, and W. Ho, *Phys. Rev. Lett.* **90** (2003) 196103.
- [10] J. Repp, G. Meyer, and K.-H. Rieder, *Phys. Rev. Lett.* **92** (2004) 036803.
- [11] T.L. Einstein, *Handbook of Surface Science*, ed. W.N. Unertl (Elsevier, Amsterdam, 1996), Vol. 1, p. 577.
- [12] J. Repp, F. Moresco, G. Meyer, K.-H. Rieder, P. Hyldgaard, and M. Persson, *Phys. Rev. Lett.* **85** (2000) 2981.
- [13] H. Knorr, H. Brune, M. Epple, A. Hirstein, M.A. Schneider, and K. Kern, *Phys. Rev. B* **65** (2002) 115420.
- [14] N. Sato, T. Nagao, and S.Hasegawa, *Phys. Rev. B* **60** (1999) 16083.
- [15] F. Silly, M. Pivetta, M. Ternes, F. Patthey, J.P. Pelz, and W.-D. Schneider, *Phys. Rev. Lett.* **92** (2004) 016101.
- [16] P. Hyldgaard and M. Persson, *J. Phys.: Condens. Matter* **12** (2000) L13.
- [17] E.J. Heller, M.F. Crommie, C.P. Lutz, and D.M. Eigler, *Nature (London)* **369** (1994) 464.
- [18] G.A. Fiete, J.S. Hersch, E.J. Heller, H.C. Manoharan, C.P. Lutz, and D.M. Eigler, *Phys. Rev. Lett.* **86** (2001) 2392.
- [19] K.W. Lau and W. Kohn, *Surf. Sci.* **75** (1978) 691.
- [20] J.S. Langer and S.H. Vosko, *J. Phys. Chem. of Solids* **12** (1960) 196.
- [21] K.A. Fichthorn and M. Scheffler, *Phys. Rev. Lett.* **84** (2000) 5371.

- [22] M. Petersilka, U.J. Gossmann, and E.K.U. Gross, Phys. Rev. Lett. **76** (1996) 1212.
- [23] A. G. Eguiluz, Phys. Rev. B **31** (1985) 3303.
- [24] I.G. Khalil, M. Teter, and N.W. Ashcroft , Phys. Rev. B **65** (2002) 195309.
- [25] G.F. Giuliani and G.E. Simion, Solid State Commun. **127** (2003) 789.
- [26] E.V. Chulkov, V.M. Silkin, and P.M. Echenique, Surf. Sci. **391** (1997) L1217; Surf. Sci. **437** (1999) 330.
- [27] V.M. Silkin, A. García-Lekue, J.M. Pitarke, E.V. Chulkov, E. Zaremba, and P.M. Echenique, Europhys. Lett. **66** (2004) 260.
- [28] J.M. Pitarke, V.U. Nazarov, V.M. Silkin, E.V. Chulkov, E. Zaremba, and P.M. Echenique, Phys. Rev. B **70** (2004) 205403.
- [29] J. P. Gauyacq, A. G. Borisov, G. Raseev, and A. K. Kazansky, Faraday Discuss. **117** (2000) 15.
- [30] A. G. Borisov, A. K. Kazansky, and J. P. Gauyacq, Phys. Rev. B **65** (2002) 205414.
- [31] M.C. Desjonquères and D. Spanjaard, Concepts in Surface Physics, Springer-Verlag, Berlin, 1996.